

# Target Studies for Mu2e-II

David Neuffer<sup>a</sup>

<sup>a</sup>*Fermilab, PO Box 500, Batavia, IL60510*

**Abstract.** In Mu2e-II 800 MeV protons at 100 kW will be used, rather than the 8 GeV 8 kW planned for Mu2e. The higher power and lower beam energy will require some significant changes in the production target. Multiple scattering is much more significant, requiring changes in the target geometry and material. Active cooling is needed and the target geometry should be modified to match the beam trajectories. Low-Z targets may be preferable because of their reduced multiple scattering and target heating effects. Production of positive secondaries ( $\pi^+$ ,  $\mu^+$ ) appears to be enhanced, suggesting that the PIP-II program should be adapted to include ( $\pi^+$ ,  $\mu^+$ ) experiments.

**Keywords:** muons, lepton conversion, targets.

## INTRODUCTION

The PIP-II accelerator [1] will provide a high-intensity 800 MeV proton beam that can be used to feed an upgraded version of the Mu2e experiment [2, 3], called Mu2e-II. The initial configuration for Mu2e-II is to replace the zmu2e incoming 8 GeV proton beam with 800 MeV PIP-II beam, while keeping the remainder of the experiment similar to the Mu2e facility, and reusing as much of the original experiment as possible [4, 5]. Figure 1 displays the technical design version of the Mu2e experiment. The different incident beam energy and much higher beam power available for mu2e-II will require some changes in this configuration. The lower-energy proton beam is more greatly deflected by the strong magnetic field, and the injected beam would not reach the target. We previously noted that the incoming 800 MeV beam trajectory could be modified to match into the mu2e target position, with relatively modest changes in the Mu2e scenario [6].

Mu2e-II plans to use much higher beam power: up to 100 kW rather than the 8 kW in Mu2e. The higher beam power will lead to more power deposited within the production solenoid, and requires modifications and improvements to the shielding within the production solenoid, in order to protect the solenoid coils from excessive heating. V. Pronskikh has studied this problem and developed some interesting possibilities for improving the shielding configurations [7, 8].

The initial target design for Mu2e was based on the use of a 16cm long, 6.3 mm diameter tungsten (W) cylinder suspended within the production solenoid, aligned to the incident proton beam, and relying on radiative cooling. Recent Mu2e studies have considered that design to be in danger of overheating and are considering significant modifications to the target design.

It was already known that radiative cooling within the Mu2e geometry would be insufficient for a 100 kW Mu2e-II beam. More recently we have noted that the Mu2e target is also not well matched to an incident 800 MeV proton beam, and would need to be modified. In this note we discuss the nature of that mismatch and suggest some variations to improve the match. We discuss some guidelines toward developing a target suitable for Mu2e-II.

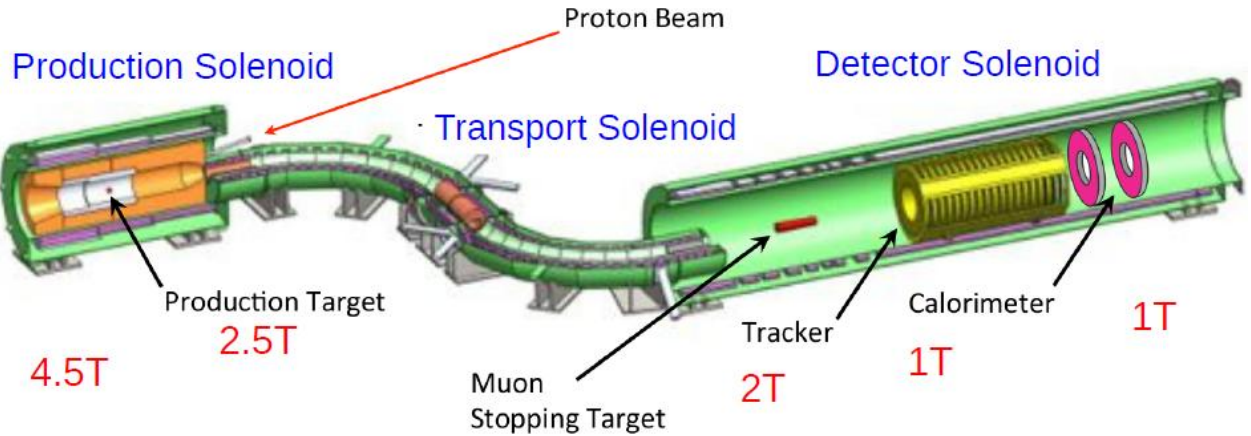


**FIGURE 1.** The mu2e Detector. Proton beam is injected off-axis toward the production target, producing secondaries that are transported to the Al stopping target.  $\mu \rightarrow e$  conversion events are detected as 105 MeV electrons in the tracker/calorimeter.

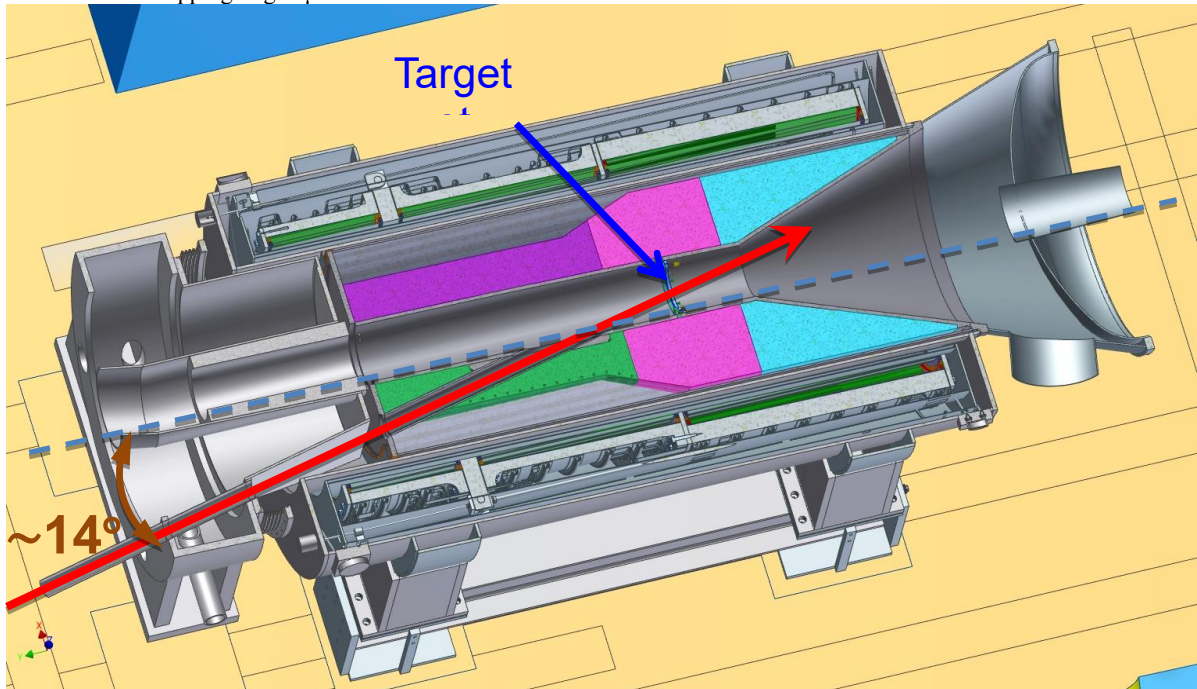


**FIGURE 2.** Entry of proton beam into the production solenoid. (from S. Werkema [11]). The bronze HRS is indicated by the green, purple, violet and cyan segments.

## TARGET CONSIDERATIONS

The me2e-II production target (PT) will have ~10 times more power incident on it than mu2e. The Mu2e baseline target is a 16cm long, 3.15 mm radius tungsten cylinder. A 7.3 kW 8 GeV proton beam deposits ~570W of energy in the target. That heatload is at a level where a free-standing radiatively cooled target could be used. The initial design for the mu2e PT is a cylinder suspended on wires within the production solenoid (see fig. 3)

Thermal calculations indicated that the temperature would reach 1700°C, which may possibly lead to excess target damage. Following analyses presented by K. Lynch, this can be reduced by changes in the target geometry. Adding fins to the cylinder to increase radiation can reduce the peak temperature to ~1400°C, but with a loss in muon yield of ~15%. A more complicated design with segmentation to reduce peak heating and obtain a more

uniform temperature distribution can reduce this to  $\sim 1100^{\circ}\text{C}$ , with a corresponding drop in yield of 30%. Final designs for implementation in mu2e have not yet been established.

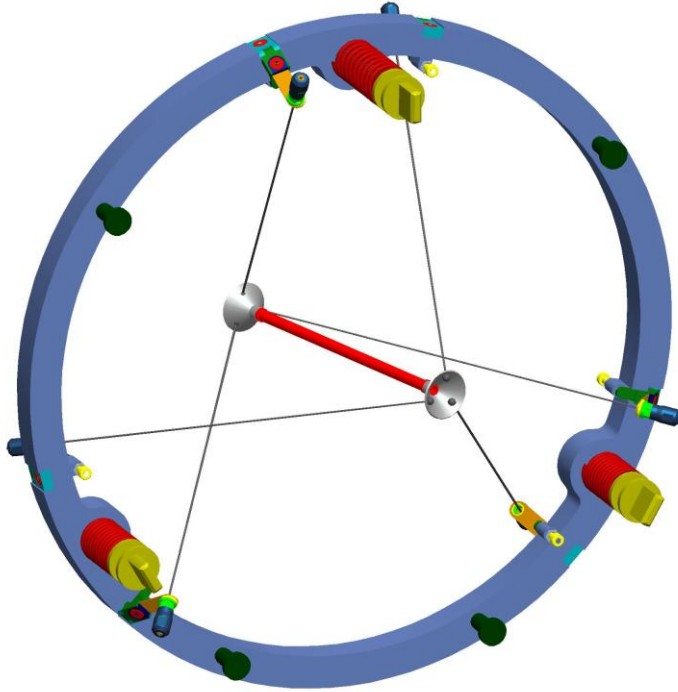


**Figure 3.** 3D view of the Mu2e target and ‘bicycle wheel’ support structure. (from TDR).

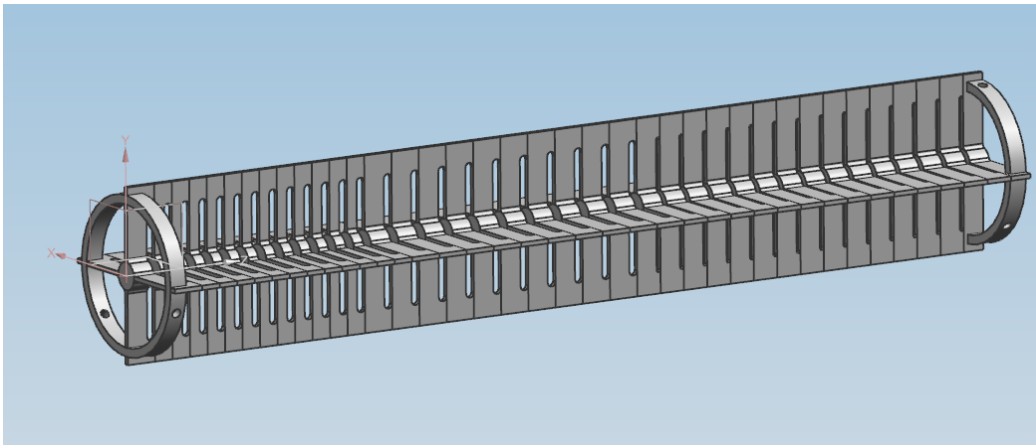


**Figure 4.** View of a segmented ‘Hangman’ W target designed for Mu2e.

8 GeV protons lose  $\sim 26$  MeV/cm in dE/ds energy loss in a W target. If the protons have a mean path of  $\sim 8$  cm, that would contribute  $\sim 190$  W to the heatload. The G4Beamline calculation of 590 W implies  $\sim 400$  W due to other processes, which would include the Pi and muon production processes.

The 100 kW 800 MeV beam for Mu2e-II would have much larger energy deposition. 800 MeV beam protons also have a dE/ds of  $\sim 26$  MeV/cm. With a 8 cm mean path in target, This would imply a heatload of  $\sim 26$  kW from dE/ds alone. Assuming that the heatload due to other processes is proportional to the beam power, and following the calculation for 8 GeV,  $\sim 5$  kW must be added, to obtain a heat load of  $\sim 31$  kW on a W target. G4Beamline simulations of the target obtain  $\sim 22.5$  kW, which is a bit less. This is more than 30 times larger than that projected for the Mu2e experiment, and will certainly require more active cooling of the target. The lower value from G4Beamline occurs because many of the protons are scattered outside the target (also reducing secondary production, see below).

Figure 5 shows energy deposition calculations for 8 GeV and 0.8 GeV beam on a tungsten target.

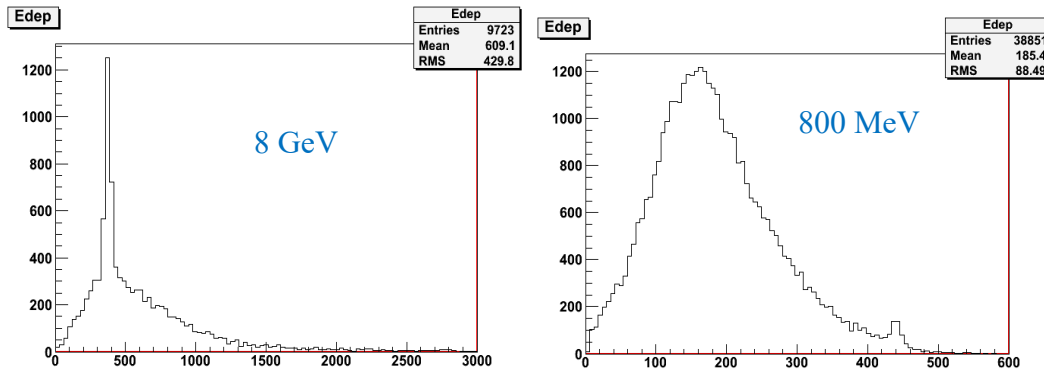


**Figure 5.** Distribution of energy deposition in a 16cm r=3.15mm cylindrical W target for 8 GeV (left) and 800 MeV (right) protons. The sharp peak at 400 MeV corresponds to 8 GeV protons that pass through with only dE/dx losses. At 800 MeV, very few protons stay within the target; most are scattered out before reaching the end of the target. Average energy loss of an 8 GeV proton is 609 MeV; average energy loss of an 800 MeV proton is 185 MeV.

In Mu2e target design, ~8 kW of 8 GeV beam was considered the limit that could be used in a radiatively cooled design. Designs for water-cooled and He-gas cooled targets were also considered for Mu2e. A water-cooled design kept peak temperatures less than ~95° C within a W or Au target, with ~50° C at the water-rod interface. A He cooled design which kept peak temperatures less than ~375° C was also developed. The gas-cooled design was extrapolated to handle 100kW of 8 GeV beam. However, the peak temperature rose to ~600° C. Also, a 100 kW 0.8 GeV beam would deposit twice as much energy as an 8 GeV beam. Significantly more design work must be done to establish an acceptable Mu2e-II target.

The dE/ds heating problem and the comparison with simulations identified an incompatibility of the W target with 800 MeV beam. The problem is that the energy loss and multiple scattering within the PT increases the incoming beam angular spread and physical size, scattering a large portion of the incident beam outside the target before it can produce secondary particles. This is a small effect with 8 GeV protons but is significant at 800 MeV.

The rms scattering angle can be estimated by:

$$\theta_{x,rms} \cong \frac{13.6 \text{ MeV}}{\beta c p} \sqrt{\frac{s}{X_0}} (1 + 0.038 \ln \left[ \frac{s}{X_0} \right]),$$

where we have included the small correction factor of  $0.038 \ln(s/X_0)$ .

$X_0$  is the material radiation length,  $s$  is distance along the target, and  $\beta c$  and  $p$  are the velocity and momentum of the proton beam. The increase in the radial beam size  $\sigma_{rms}$  is:

$$\sigma_{rms} \cong \sqrt{\frac{2}{3}} \frac{13.6 \text{ MeV}}{\beta c p} s \sqrt{\frac{s}{X_0}} (1 + 0.038 \ln \left[ \frac{s}{X_0} \right])$$

$\sigma_{rms}$  is 3.8 mm at  $s=8$  cm, greater than the PT radius of 3 mm, and is ~1.1cm at  $s = 16$ cm. The mean nuclear interaction length is ~10 cm in W, indicating that a significant number of protons would have exited the target before producing secondaries. This could be mitigated by using a larger-radius target, but that would increase loss of secondaries produced at small radius from reabsorption and energy loss before exiting the target. That could be partially mitigated by tapering the PT radius to follow the beam size. In any case, the calculation indicates that the Mu2e PT is not properly matched to a 800 MeV beam and a redesign is indicated.

$\theta_{x,rms}$  is ~0.085 radians at  $s=16$ cm which gives the beam exiting the target a large divergence. The problem is much less significant for 8 GeV protons, where we obtain  $\sigma_{rms} = 0.156$  cm, and  $\theta_{x,rms} = 0.012$ .

The dE/ds heating and multiple scattering can be reduced by using a lower-Z target, and a lower density target could also have a larger radius without increasing reabsorption. Table XX displays some key parameters of possible target elements, as well as scattering parameters at  $z=16$  cm and  $z= \lambda_{int}$ . The lighter elements have much reduced scattering effects. A practical option could be an  $r=1$ cm  $L= \sim 40$ cm C target or other material. An important advantage of the low-Z target is the reduced multiple scattering angle ( $<1^\circ$ , similar to that for the 8 GeV beam). The smaller value will make it possible to direct much of the initial beam energy into a compact beam dump, similar in radius to that used for Mu2e.

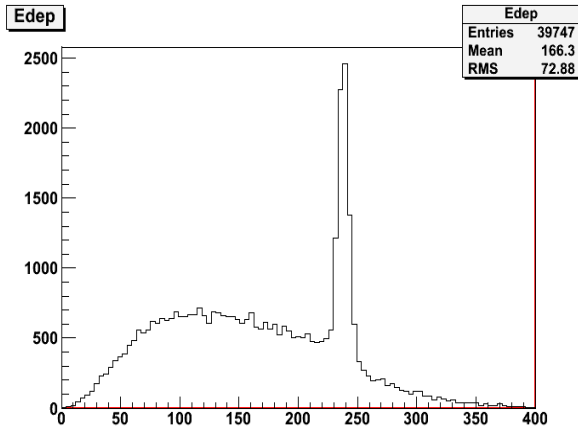


**Figure 6.** Distribution of energy deposition in a 50cm long,  $r=10$ mm cylindrical C target for 800 MeV protons. The sharp peak at 240 MeV corresponds to 800 MeV protons that pass through with only  $dE/dx$  losses. Average energy loss of an 800 MeV proton is 166 MeV.

This reduction in multiple scattering is mitigated to some extent by the large-angle nuclear scattering in a low- $Z$  material. Thus a simulation using a C target (50cm long, 1.2cm radius) produces outgoing beam with a core with rms 1cm, but with an extended halo of large-angle scattered protons. The scattering is much less than that for a W target. The exiting protons have an rms scattering angle of  $\sim 1^\circ$ , compared to  $\sim 5^\circ$  with W [see fig. 7].

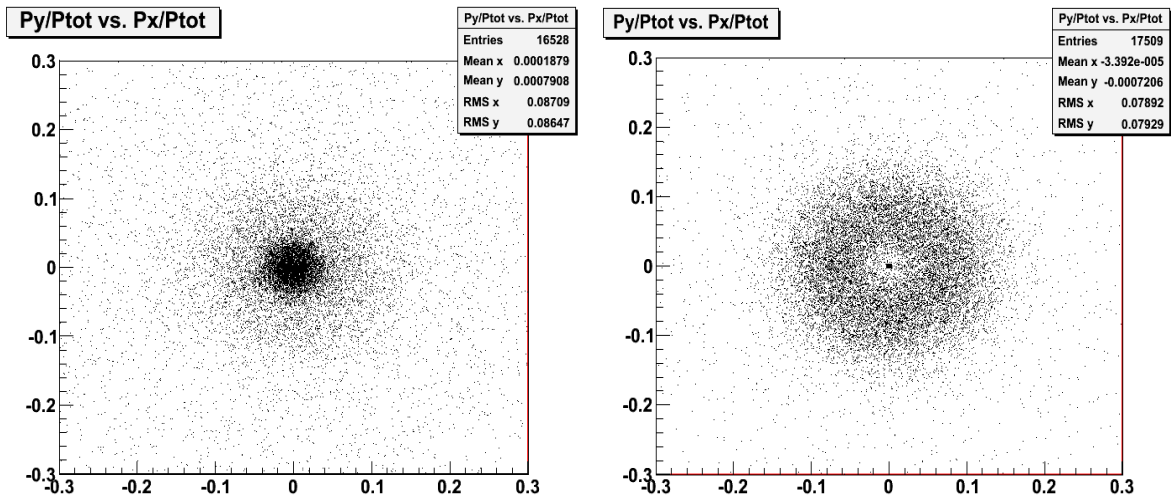


**Figure 7.** Transverse momentum distributions of proton beam exiting a 50 cm C target (left) and a 16 cm tungsten target (right). The incident beam was 800 MeV protons. The exiting protons have an rms scattering angle of  $\sim 1^\circ$  from C, compared to  $\sim 5^\circ$  with W.

The simulations shows that the incident proton beam remains largely within the C target and is not scattered outside of it by multiple scattering. The  $\pi/\mu^-$  production of the lower  $Z$  targets must be checked, as it may be less. A more complete comparison using the full mu2e simulation model is needed. Intermediate  $Z$  elements (Ti, Fe, ...) would also have less scattering outside the target but might also have greater  $\pi/\mu$  production than low- $Z$ , but more complete simulations will be needed to see if there is a final production target optimum that is not a high- $Z$  material. Some initial calculations toward determining a production optimum are discussed in the next section.

Element	Density	$X_0$ (cm)	dE/ds(min)	$\lambda_{int}$ (cm)	$\sigma_{rms}(16)$	$\sigma_{rms}(\lambda_{int})$	$\theta_{x,rms}((\lambda_{int}))$
Be (4,9)	1.848	35.3	2.95	42.0	0.096	0.425	0.012
B <sub>4</sub> C (5.2,11.2)	2.52	20.4	4.59	32.56	0.126	0.375	0.014
C (6,12)	2.0	17.5	3.5	42.8	0.13	0.52	0.016
Al (13,27)	2.7	8.9	4.36	39.7	0.20	0.82	0.025
Ti (22,47.8)	4.54	3.56	6.70	27.8	0.33	0.77	0.033
Fe (26,55.8)	7.87	1.76	11.4	16.8	0.482	0.52	0.037
Cu(29,63.55)	8.96	1.44	13.7	15.3	0.536	0.50	0.039
W (74, 184)	19.3	0.35	22.1	9.9	1.14	0.55	0.066

## SIMULATION STUDIES OF TARGET CONFIGURATIONS

We considered several other possible targets, particularly those using low and intermediate-Z. In initial simulations, we represented the targets as straight cylinders, with beam incident on the base of the cylinders. The targets are at the 14° inclination chosen for mu2e and centered at the reference location. The target lengths were chosen to provide a similar number of interaction lengths (~1.5) as the baseline W target. The targets are placed within the production solenoid (PS) geometry and fields, and particles that reach the exit of the PS, entering the transport solenoid(TS), are evaluated.

The calculated rates were obtained using G4Beamline [12], but with the constraints that only p,  $\pi^\pm$ , and  $\mu^\pm$  are saved, which greatly increases computing speed. Some  $\pi$ , and  $\mu$  from tertiary production (involving n, e, K,...) would be missed, so the numbers are probably a bit smaller than in a complete simulation. We are including  $\pi$  and  $\mu$ , since  $\pi$  decay can produce  $\mu$ 's that will stop in the target.

**Table 2:** Initial production rate calculations for cylindrical targets. The production is evaluated at the entry to the TS (exit of the PS), and has not been corrected for the bending of the entering proton beam.

Material	L	r (cm)	$\mu^-/p \cdot 10^{-3}$	$\pi^-/p \cdot 10^{-3}$	$\mu^+/p \cdot 10^{-3}$	$\pi^+/p \cdot 10^{-3}$
<b>C</b>	50	1.2	1.0	1.31	4.27	5.78
<b>B<sub>4</sub>C</b>	40	0.8	1.18	1.55	6.48	7.41
<b>Ti</b>	40	1.0	0.84	1.19	3.45	4.05
<b>Fe</b>	24	0.6	0.82	1.02	3.65	3.96
<b>W</b>	16	0.315	1.39	1.53	3.82	3.98
<b>W/10 8GeV</b>	16	0.315	2.14	2.53	2.03	2.38

In these results there is a decrease in the  $\mu^-$  and  $\pi^-$  by ~33% from an 8 GeV beam at comparable power. Lighter-Z atoms appear to provide a bit less than W at the PS exit, with apparently worse production for intermediate-Z targets. Lower-Z (C and B<sub>4</sub>C) appears somewhat favored.

Another difference is that the production of positives ( $\pi^+$ ,  $\mu^+$ ) appears to be much larger than that of negatives ( $\pi^-$ ,  $\mu^-$ ). For low-Z targets the positives production appears to ~6× as large. This is unlike the case for 8 GeV incident protons, where positives and negatives are nearly equal.

## Magnetic deflection within the target

The 800 MeV proton beam ( $P=1.463$  GeV/c) is somewhat deflected by magnetic fields as it passes through the target and is therefore mismatched to the straight targets. A curved target matched to the deflection of the incident proton beam should be used instead of a straight cylinder.

The expected deflection can be calculated using the equations of motion:

$\vec{F} = e\vec{v} \times \vec{B}$ , with  $\vec{B} \cong B_0 \vec{e}_z$  and  $B_0 = 4$ T. The initial velocity is  $\beta c (\sin \theta \vec{e}_x + \cos \theta \vec{e}_z)$ , where  $\theta$  is the angle on target ( $14^\circ$  in the baseline case). The net force is vertical with a displacement given by  $\delta y \cong \frac{1}{2} \sin \theta \frac{B_0}{B\rho} z^2 \cong 0.1z^2$ . At the

end of a 40 cm target the beam would be displaced by 1.6cm. Bending the target by this amount keeps the proton beam within the target, and increases the number of secondaries produced. The bend can be obtained by a segment of a torus with radius of  $B\rho/(B_0 \sin(\theta)) = \sim 5.04$  m.

Applying this adjustment to the  $B_4C$  example increases the number of secondaries produced at the PS exit to  $\sim 1.41 \times 10^{-3} \mu^-/p$ ,  $\sim 1.75 \times 10^{-3} \pi^-/p$ . These are a bit higher than the W production values. With a 50cm C target, these numbers are  $\sim 1.21 \times 10^{-3} \mu^-/p$ ,  $\sim 1.56 \times 10^{-3} \pi^-/p$ .  $B_4C$  production is a bit better for production of negatives, possibly because of the larger number of neutrons in the target as well as the higher density. C appears to be slightly better for positives production. While C has been commonly used in production targets,  $B_4C$  has not yet been developed for this application. Berg et al. have noted production improvements from  $B_4C$ , encouraging its development [13].

**Table 3:** Initial production rate calculations for cylindrical targets, bent to follow the baseline proton beam trajectory. (The W values were not rerun because of the small correction. The production is evaluated at the entry to the TS (exit of the PS).

Material	L	r (cm)	$\mu^-/p \cdot 10^{-3}$	$\pi^-/p \cdot 10^{-3}$	$\mu^+/p \cdot 10^{-3}$	$\pi^+/p \cdot 10^{-3}$
C	50	1.0	1.21	1.56	7.16	8.69
$B_4C$	40	1.0	1.41	1.75	7.01	8.06
Ti	40	0.8	0.87	1.15	3.66	4.98
Fe	30	0.6	0.82	1.02	3.65	3.96
Ni	30	0.6	0.83	0.90	3.69	4.06
W	16	0.315	1.39	1.53	3.82	3.98
W/10 8GeV	16	0.315	2.14	2.53	2.03	2.38

## CONCLUSIONS

The lower energy PIP-II proton beam (800 MeV) has relatively enhanced  $dE/ds$  energy losses and multiple scattering, particularly in high-Z targets. A W target at mu2e parameters (16cm long and 3.15mm radius) would scatter much of the incident proton beam outside the target. A low-Z target (C or  $B_4C$ ) would have lower beam energy loss and lesser scattering limitations. A simplified first evaluation indicates that production of ( $\mu^-$ ,  $\pi^-$ ) would be similar to that of the W target. Intermediate-Z targets (Ti, Fe) appeared to have somewhat less secondary production than low-Z and high-Z cases. ( $\pi^+$ ,  $\mu^+$ ) production from 800 MeV beam appears to be relatively enhanced, particularly from low-Z targets. Experiments on positives ( $\pi^+$ ,  $\mu^+$ ) should be included in the PIP-II era.

## ACKNOWLEDGMENTS

We thank D. Glenszinski, R. Bernstein, V. Pronskikh and J. Miller for helpful discussions. This manuscript has been authored by Fermi Research Alliance, LLC under Contract No. DE-AC02-07CH11359 with the U.S. Department of Energy, Office of Science, Office of High Energy Physics.

## REFERENCES

1. M. Ball et al., The PIP-II Conceptual Design Report (2017).
2. Bartoszek, L. et al., Mu2e Technical Design Report, Mu2e Doc 4299, arXiv 1501.0524.(2015).
3. Mu2e Conceptual Design Report, Mu2e Document 1169-v12 (2012).
4. K. Knoepfel et al., “Feasibility Study for a Next-Generation Mu2e Experiment”, arXiv:1307.1168v2 (2013).
5. F. Abusalma et al., “Expression of Interest for Evolution of the Mu2e Experiment”, Mu2e docdb-10655, Feb. 18, 2018.
6. D. Neuffer, “Mu2e-II Injection from PIP-II”, Fermilab TM-2677-AD-APC, April, 2018.
9. K. Lynch, “Production Target Issues and Plans”, Mu2e-doc-24232, Feb. 2019.
10. K. Lynch, “Energy deposition in Mu2e-like production targets with protons from 800 MeV to 8 GeV”, Mu2e-doc-8376 June, 2017.
11. PDG Review of Particle Physics, K. Nakamura et al. (Particle Data Group), J Phys. G37, 075021 (2010).
12. T. Roberts et al., Muons, Inc., G4BeamLine 3.06 (2018), <http://www.muonsinc.com/muons3/G4beamline>.
13. F. Berg et al., “Target studies for surface muon production”, Phys. Rev. Accel. and Beams 19, 024071(2016).